AWARD NUMBER: W81XWH-16-1-0375

TITLE: SERS Nanosensors for in Vivo Glucose Sensing

PRINCIPAL INVESTIGATOR: Richard Van Duyne

CONTRACTING ORGANIZATION: Northwestern University
Chicago, IL 60611

REPORT DATE: September 2018

TYPE OF REPORT: Annual Report

PREPARED FOR: U.S. Army Medical Research and Materiel Command
Fort Detrick, Maryland 21702-5012

DISTRIBUTION STATEMENT: Approved for Public Release;
Distribution Unlimited

The views, opinions and/or findings contained in this report are those of the author(s) and should not be construed as an official Department of the Army position, policy or decision unless so designated by other documentation.

# REPORT DOCUMENTATION PAGE

*Form Approved*
*OMB No. 0704-0188*



| **1. REPORT DATE** | **2. REPORT TYPE** | **3. DATES COVERED** |
|---|---|---|
| September 2018 | Annual report | 1 Sep 2017- 31 Aug 2018 |

**4. TITLE AND SUBTITLE**

SERS Nanosensors for in Vivo Glucose Sensing

**5a. CONTRACT NUMBER**
W81XWH-16-1-0375

**5b. GRANT NUMBER**

**5c. PROGRAM ELEMENT NUMBER**

**6. AUTHOR(S)**

Richard Van Duyne, Ji Eun Park, Emma Vander Ende

E-Mail: vanduyne@northwestern.edu

**5d. PROJECT NUMBER**

**5e. TASK NUMBER**

**5f. WORK UNIT NUMBER**

**7. PERFORMING ORGANIZATION NAME(S) AND ADDRESS(ES)**

Northwestern University
Evanston, Illinois 60208

**8. PERFORMING ORGANIZATION REPORT NUMBER**

**9. SPONSORING / MONITORING AGENCY NAME(S) AND ADDRESS(ES)**

U.S. Army Medical Research and Materiel Command
Fort Detrick, Maryland 21702-5012

**10. SPONSOR/MONITOR'S ACRONYM(S)**

**11. SPONSOR/MONITOR'S REPORT NUMBER(S)**

**12. DISTRIBUTION / AVAILABILITY STATEMENT**

Approved for Public Release; Distribution Unlimited

**13. SUPPLEMENTARY NOTES**

**14. ABSTRACT**

The goal of this program is to develop small and sensitive nanosensors for the continuous glucose monitoring in living tissue without the need for drawing blood. A major advantage of the transdermal sensors we are developing is to directly detect glucose itself – not the byproducts of its transformation. The technique we use – surface-enhanced Raman spectroscopy (SERS) – is based on light and informs on the presence of glucose on or near metallic nanosensors. **In Year 1**, we have worked on the development of i) sensitive nanosensors, ii) selective capture layers that can be immobilized onto metal surfaces, and iii) the integration of both. We have successfully developed a novel SERS nanoplatform that integrates gold nanorods with biocompatible hydrogels of variable stiffness. The fabrication of SERS-active microneedle patches has been successfully initiated and demonstrated over the first 12 months of the program using stiff hydrogels. Several approaches have been taken and validated against SERS activity. We have shown that water-soluble molecules can diffuse through the hydrogel pores and be detected in the mM range, where glucose is physiologically relevant. **In Year 2**, we have implemented the glucose-capture ligand on the gold nanord surface that are already integrated with the microneedle patches. The stability of the nanorods in buffer conditions as well as organic solvents was evaluated. Additionally, SERS activity and device performance were investigated on a skin phantom. The plasmonic patch fabrication protocols were modified in such a way that the SERS activity can be selectively localized at the microneedle's tip. Extended studies on sensing measurements and theoretical calculations were done on evaluating boronic acid derivatives for glucose recognition. Finally, the plasmonic microneedle patches were validated as a SERS-based biosensing device by measuring reversible pH change from solution.

**15. SUBJECT TERMS**

Glucose, sensing, boronic acid, SERS, spectroscopy, hydrogel, microneedle array, continuous glucose monitoring, medical device

| **16. SECURITY CLASSIFICATION OF:** | | | **17. LIMITATION OF ABSTRACT** | **18. NUMBER OF PAGES** | **19a. NAME OF RESPONSIBLE PERSON** |
|---|---|---|---|---|---|
| **a. REPORT** | **b. ABSTRACT** | **c. THIS PAGE** | Unclassified | 28 | USAMRMC |
| Unclassified | Unclassified | Unclassified | | | **19b. TELEPHONE NUMBER** *(include area code)* |

**Standard Form 298 (Rev. 8-98)**
**Prescribed by ANSI Std. Z39.18**

## Table of Contents

**Page**

1. INTRODUCTION

Diabetes is a chronic disease in which levels of blood glucose – a small molecule that serves as an energy source – exceed the norm and pose a host of primary and secondary health complications. The goal of this program is to lighten the physical and psychological burden that daily blood glucose checks represent for patients and to improve their long-term health through the development of small and sensitive nanosensors that *continuously* detect and measure glucose in living tissue over a long period of time (several months) without the need for drawing blood. A major advantage of the transdermal sensors we are developing is to *directly* detect glucose itself – not the byproducts of glucose transformation - which require external reagents that add extra costs and steps, and which can respond to other molecules in the blood, such as fructose, leading to false inflation of measurements.

2. KEYWORDS

Glucose, diabetes, sensing, biosensing, boronic acid, SERS, Raman scattering, spectroscopy, hydrogel, microneedle array, plasmonic microneedles, transdermal patch, continuous glucose monitoring, medical device

3. ACCOMPLISHMENTS

**Major goals of the project**
As stated in the approved Statement of Work (SOW), the four major goals of Year 2 of this program were:

1- **Synthesis of anti-biofouling layers** led by Site 2 (Mrksich lab).
We proposed to synthesize and incorporate polymeric coatings with anti-biofouling property over Au nanorods (AuNRs). Instead of synthesizing additional hydrogel coatings on gold nanorods (AuNRs), we chose to encapsulate AuNRs with Gantrez-PEG hydrogels and fabricate plasmonic microneedles.
2- **Demonstrate 3 months stability of biocompatible, anti-biofouling coatings in complex biofluid** carried out by both Site 1 and 2 (Van Duyne and Mrksich labs).
Additional material we proposed to fabricate microneedles with was Norland Optical Adhesive (NOA) polymer. After fabricating plamonic NOA microneedles with AuNRs, we investigated the stability of the microneedle sensor over a month period in buffer solution.
3- **Integration with functional nanosensors and SERS evaluation**, carried out by both Sites 1 and 2 (Van Duyne and Mrksich labs).
We proposed a boronic acid-based glucose capture layer and several molecular designs were synthesized and investigated for their efficiency to bind glucose. In addition to evaluating various glucose capture ligands, we worked on optimizing NOA microneedles for SERS biosensing and developing a method for localizing AuNRs on the microneedle tips.
4- ***Ex vivo* glucose sensing by SERS; demonstrate 3 months stability and functionality of the sensor** carried out by both Site 1 and 2 (Van Duyne and Mrksich labs).
Although there was a delay in the project due to investigating boronic acid capture ligands for glucose binding, we successfully fabricated plasmonic NOA microneedles. We decided to evaluate the functionality of this SERS nanoplatform for a control yet biologically relevant metric: pH. We successfully obtained a pH calibration curve within pH range 2 to 12. We then detected pH of a skin phantom (agar gel) and validated the mechanical stability by puncturing the microneedles on the gel.

## 1- Synthesis of anti-biofouling layers

Over this second year we worked extensively on developing SERS-active microneedle arrays for a transdermal sensor for continuous glucose monitoring (CGM). The basic structural parameters that dictate the effectiveness of such a sensor are optical transparency at the wavelength of the SERS excitation in the 700-800 nm region, robust design to effectively penetrate through skin retaining the structural integrity and functionality, both chemically and mechanically stable throughout the sensing time period, and depth of the microneedles in direct contact with the interstitial fluid which will minimize the contamination and biofouling risks of the microneedles from blood-borne proteins. We chose two different polymeric materials for fabricating microneedles, which are Gantrez-poly(ethylene glycol) (Gantrez-PEG) hydrogels and Norland Optical Adhesive (NOA). Gantrez is a non-toxic material that exhibits antimicrobial properties when mixed with PEG.[1] Donnelly et al. demonstrated the capability of Gantrez-PEG based microneedles for drug delivery and biosensing applications *in vivo*.[2] The selection of this hydrogel material relies on the mechanical robustness to penetrate skin, porosity for diffusion, biocompatibility, and optical characteristics of the solidified hydrogel. In addition to Gantrez-PEG hydrogels, NOA materials are optically transparent which makes them a good candidate for transdermal biosensors. Once photocured, they form mechanically robust structures with high stiffness (~ GPa range).

### 1.1 Summary of solid microneedles arrays

Solid microneedles arrays were fabricated via a replica molding method using two different classes of polymeric materials: (i) Gantrez-PEG hydrogels and (ii) NOA-based rigid polymers. A plasmonic component (Au nanorods, or AuNRs) was incorporated to make the microneedles SERS active by either embedding the AuNRs in the solid microneedles or through physisorption on the surface of the microneedles, depending on the microneedle material type as well as the fabrication method. For example, AuNRs can only be incorporated into the hydrogel matrix by pre-mixing the AuNRs with the pre-polymer mixture prior to crosslinking. Although the hydrogel swells in water, the mesh size is not large enough and diffusion of the AuNRs into the matrix is severely limited. AuNRs also do not readily localize to the tips of the microneedles where plasmonic enhancing is most relevant. Additionally, NOA pre-polymer mixtures are very viscous liquids that prevent incorporation of AuNRs with a homogeneous dispersion. Therefore, plasmonic particles can only be localized on the NOA surface following the microneedle fabrication. Finally, Raman reporter molecules (glucose capture ligands) are assembled in the self-assembled monolayer (SAM) form on the surface of AuNRs via ligand exchange with the particle stabilizing ligand, cetyltrimethylammonium bromide (CTAB). In the following subsections, we describe the details of how Raman reporter molecules were assembled with the hydrogel and NOA-based solid microneedles, the current challenges for fabrication methods, resulting SERS activities and our proposed solutions to address some of the issues that we encountered.

### 1.2. Background of Gantrez-PEG hydrogel (anti-biofouling property)

Gantrez is a synthetic, alternating copolymer of maleic anhydride and methyl vinyl ether. Gantrez and its acidic form have been used in various biomedical applications such as thickening agents in ointments, denture adhesives and drug carriers for oral drug delivery systems.[3,4] Although there is limited information in the literature about extensively studied biocompatibility, there are some research work demonstrating no adverse effects of Gantrez hydrogels using in vitro and in vivo biocompatibility tests.[5,6] To test the biocompatibility of the Gantrez hydrogel-based microneedles,

we plan to perform cell culture on the surface of microneedles and investigate the cellular viability.

### 1.3 SERS active solid hydrogel-based microneedles

Solid hydrogel-based microneedles were prepared by casting the aqueous mixture of Gantrez, PEG and AuNRs on a PDMS mold and polymerizing at high temperature (80°C) via esterification of carboxyl and hydroxyl groups in Gantrez and PEG, respectively. Then, the resulting microneedle patch is submerged in a glucose-capture ligand solution to induce the ligand exchange with CTAB and to generate SAMs of Raman reporter molecules on the AuNR surfaces. **Figure 1** demonstrates the SERS activity of plasmonic hydrogel microneedles through detecting Raman fingerprints of commercially available boronic acid-based glucose capture ligand (4-mercaptophenyl boronic acid, 4-MPBA) at 1074 and 1588 $cm^{-1}$ in a pH 10 buffer. The control sample that was swollen in the working buffer condition (pH 10) in the absence of 4-MPBA does not show any Raman fingerprints overlapping with the Raman spectrum of reporter molecule. After glucose was incorporated into the swelling buffer, even at very high concentration (1 M), we could still measure the SERS signals of the reporter molecule, indicating that the reporter molecule is robust enough for this experiment. The purpose of the glucose-capturing Raman reporter is to either bring glucose close enough to the surface of the Raman signal enhancing AuNRs that it can be directly detected (i.e., Raman peaks of glucose would appear), or to indirectly report the presence of glucose through spectral changes (e.g., peak position shifting). Of the two, the former is more difficult to achieve owing to the sharp distance dependence of SERS.[7] However, we see no direct evidence of glucose after 4-MPBA incubation in 1 M glucose, and the characteristic peaks at 1074 and 1588 $cm^{-1}$ maintain their positions upon glucose addition.

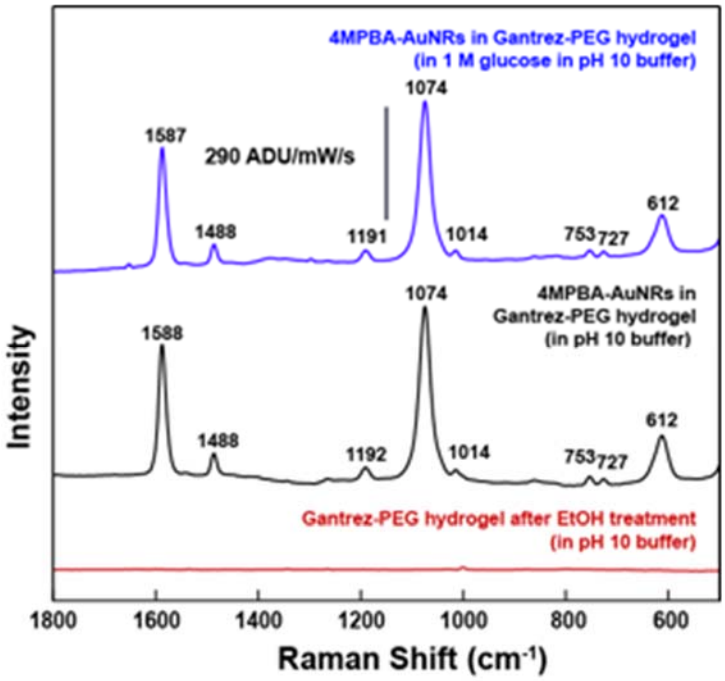


**Figure 1. SERS activity of plasmonic-PEG hydrogel.** SERS spectra 4-MPBA localized in the flat plasmonic Gantrez-PEG hydrogel before (black) and after (blue) glucose introduction. Control sample does not include AuNRs within the hydrogel matrix (red) ($\lambda_{ex}$ = 785 nm, 20x ELWD objective, $P_{ex}$ = 278 μW, Savitsky-Golay filtering and baseline correction).

The greatest challenge in preparing plasmonic hydrogel-based microneedles is the capture ligand implementation step where dried hydrogel patch, into which AuNRs are already incorporated, is exposed to capture ligands in organic solvent. Some glucose capture ligands, which show greater promise for glucose detection than 4-MPBA, are only sufficiently soluble for functionalization in

organic solvents. In addition to solvent exposure during capture ligand immobilization, plasmonic hydrogel microneedles will be interacting with interstitial fluid upon piercing in skin which is estimated to be a prolonged time period for biosensing and gives enough time to get fully swollen. These two factors – multiple swelling steps with different solvents, and long term swelling in interstitial fluid - brought into question whether the AuNRs will remain intact within the hydrogel matrix. Therefore, it was important to investigate the entrapped AuNR stability within the Gantrez-PEG hydrogel patch under organic and aqueous solvent conditions.

We used the UV-Vis extinction of AuNRs to evaluate the presence of entrapped particles in the hydrogel patch. To test the particles stability, a slab of flat plasmonic hydrogel was incubated in ethanol for 1 hour and then dried. UV-Vis spectra of the dry hydrogel before and after ethanol treatment shows no change in the extinction peaks at 500-600 nm and 800 nm regions (**Figure 2**-blue and orange spectra) that are characteristic longitudinal and transverse surface plasmon extinction peaks for the 50 nm long and 20 nm wide AuNRs that we use. This represents that AuNRs are still in the hydrogel matrix with minimum particle loss via diffusion which is below the optical detection limits. Then, the sample was soaked in DI water for 1 h. This time, the wet sample's UV-Vis extinction was measured because the longterm goal is to take biosensing measurements through the swollen plasmonic hydrogel microneedles which have pierced skin. We observed a significant decrease in the peak intensities in the UV-Vis spectrum. This may mean either (i) particles already leached out of the hydrogel matrix as the hydrogel swelled or (ii) the density of particles was diminished in a given volume with the geometrical expansion effect of swelling. Once the sample was dried, the extinction peaks were recovered. We have seen a very similar trend in the extinction spectrum upon swelling in a basic buffer condition (pH 10) which is the working buffer condition for glucose capturing with 4-MPBA. Thus, we concluded that AuNRs are physically locked within the Gantrez-PEG hydrogel and remain in the matrix as the hydrogel swells with organic and aqueous solvents.

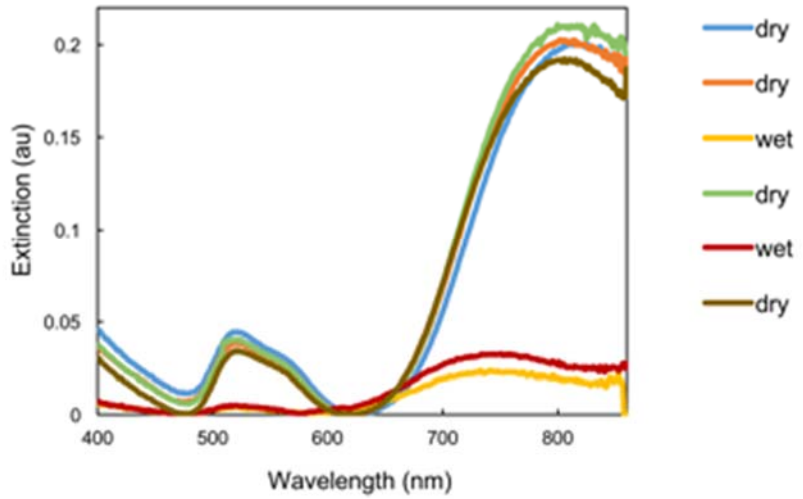


**Figure 2. Au NRs stability within plasmonic hydrogel upon solvent (ethanol, DI water, and pH 10 buffer) exposure.** UV-Vis spectra of flat plasmonic Gantrez-PEG hydrogel in (dry-blue) dried form right after preparation, (dry-orange) dried form after swelling in ethanol, (wet-yellow) swollen with DI water, (dry-green) dried form after DI exposure, (wet-red) swollen in pH 10 buffer, (dry-brown) and dried after buffer exposure.

Although we observed with UV-Vis measurements that AuNRs are stable in the hydrogel matrix during solvent treatment in a fully soaked condition, we also observed that the patch does not go back to its original flat 3D geometry due to non-uniform shrinkage of two surfaces. We didn't see any change in mechanical robustness for the samples that went through swell-dry cycle as evidenced by initial punching tests using skin mimicking agarose gel phantom. However, hydrogel microneedles

with wrinkles may prevent maximum engagement with the skin and this may lead partial penetration of the microneedles that will negatively impact the sensing measurements. One way of resolving this issue would be to functionalize AuNRs with SAMs of Raman reporter molecules prior to particles incorporation into the Gantrez-PEG hydrogel. Thus, the patch will not go through a post-processing with solvent and the structural integrity would be maintained.

### 2- Demonstrate 3 months stability of biocompatible, anti-biofouling coatings in complex biofluid

Similar to evaluating AuNRs stability within plasmonic Gantrez-PEG patch under organic and aqueous solvent conditions, it is crucial to define the particles stability of plasmonic NOA microneedles and corresponding SERS activity in a biofluidic mimic considering the skin pierced patch. The exact composition of interstitial fluid is still a subject of study, but its known components include small and large molecules such as metabolites (glucose, lactate, glutamate), ions ($Na^+$ and $K^+$), cytokines, and proteins.[8] Therefore, we used PBS buffer solution as the interstitial fluid mimicking condition to determine the particles stability. The plasmonic NOA patch was incubated in the PBS buffer for an extended time period (one month) and their optical extinctions were used to evaluate the presence of AuNRs assembly on the patch surface (**Figure 3**). The results are promising – we demonstrate particle stability and SERS activity under one month in PBS buffer.

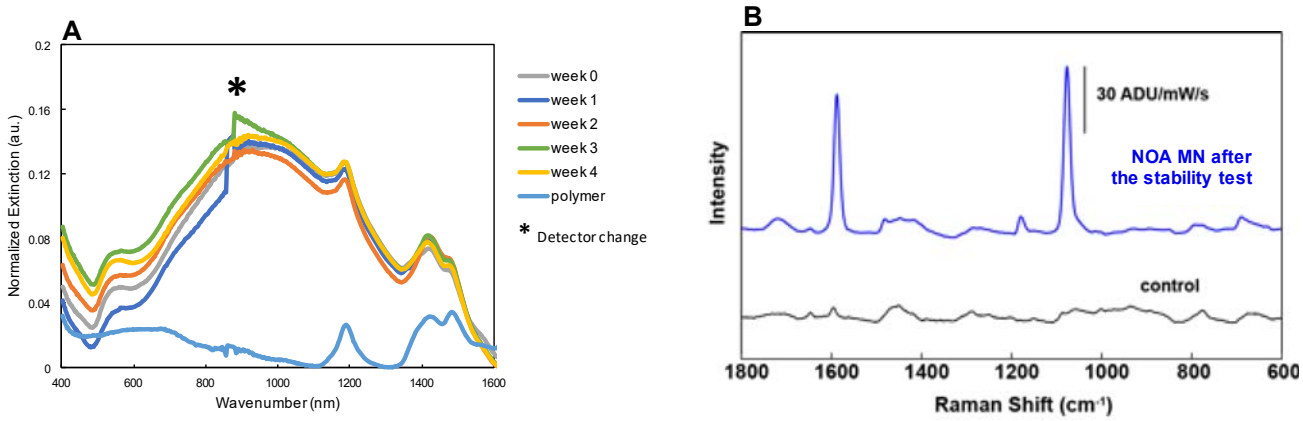


**Figure 3. Monitoring Au NRs stability and SERS activity of plasmonic NOA microneedles in interstitial fluidic mimicking condition.** (A) UV-Vis spectra of AuNRs and (B) SERS spectra of a Raman reporter (4-mercaptobenzoic acid, 4-MBA) on the plasmonic NOA microneedles surface before and after incubating in PBS buffer for a one month period. Control sample does not include the reporter molecules on the AuNRs surfaces.

### 3- Integration with functional nanosensors and SERS evaluation

We proposed to use boronic acid-based glucose capture ligand. We tried minimizing the distance between the boronic acid receptor and the surface-binding thiol by using a smaller size boronic acid-based molecule compared to a bisboronic acid. SERS is distance dependent and we can maximize the Raman signal enhancement with a small size glucose capture ligand. Along with evaluating monoboronic acid derivatives for glucose recognition, we worked on optimizing NOA microneedles for SERS biosensing and developed a method to localize AuNRs at microneedle tips.

#### 3.1. Evaluating monoboronic acid derivatives for glucose recognition

Phenylboronic acids (PBAs) are small molecules widely reported to reversibly bind glucose. The mechanism through which PBAs interact with glucose is an esterification of the hydroxyl groups

of the diols through bonding with the boron of the PBA, further forming cyclic boronate esters. Boronic acids can exist in either neutral trigonal forms or anionic tetrahedral forms, depending on the pH of the environment. The binding constant of anionic tetrahedral boronate ester for glucose is higher than that of the trigonal boronate esters. Thus, the $pK_a$ of the PBA should ideally be lower than the pH of the environment.[9]

To understand the binding interaction of PBAs with glucose and quantitatively detect glucose using SERS, 4-mercaptophenylboronic acid (4-MPBA), the simplest and commercially available PBA, was used. In addition to 4-MPBA, we also used fluorinated 4-MPBA synthesized in the Mrksich lab to investigate glucose binding. With the electron-withdrawing fluorine group, the fluorinated 4-MPBA (Figure 1B) allows sensing glucose at physiological pH.

### a. 4-MPBA and fluorinated 4-MPBA

Density functional theory (DFT) calculations of the normal Raman of 4-MPBA with and without glucose binding show clear spectral changes of 4-MPBA upon glucose binding (**Figure 4**). We then verified the binding interaction with glucose in solution. To determine the glucose binding constant ($K_a$) of 4-MPBA in solution, a UV-visible spectrophotometric titration study was done by varying the concentration of glucose (0-900 mM) at a constant 4-MPBA concentration in pH 10 buffer (**Figure 5A**). With a $pK_a$ value of 9, the binding interaction of 4-MPBA with glucose works best in basic conditions.[9] As the concentration of glucose increased the shoulder peaks at 263 nm and 292 nm increased and decreased, respectively. As shown in **Figure 5B**, the data was fitted to a Langmuir isotherm model and the binding constant of 4-MPBA for glucose in pH 10 was determined to be 90 $M^{-1}$. To check the glucose binding interaction on the surface, SERS of 4-MPBA functionalized on a plasmonic substrate was measured in pH 10 buffer solution and saturated glucose solution in a flow cell (**Figure 5C**). A new peak at 1574 $cm^{-1}$ appeared in the SERS spectrum taken in pH 10 buffer. This peak represents the anionic tetrahedral-form of boronic acid.[10] However, no glucose Raman peaks (direct evidence) or peak shifts (indirect evidence) in the SERS data was observed upon introducing saturated glucose solution. SERS of fluorinated 4-MPBA before and after introducing glucose solution also did not show direct or indirect evidence of glucose binding.

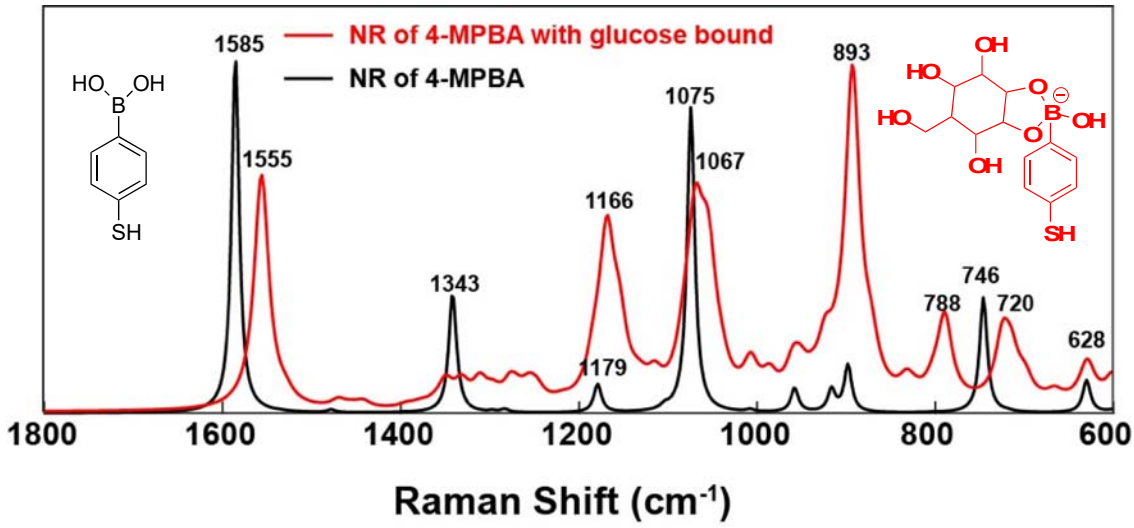


**Figure 4. DFT calculations for normal Raman of 4-MPBA complexed with (red) and without (black) glucose.**

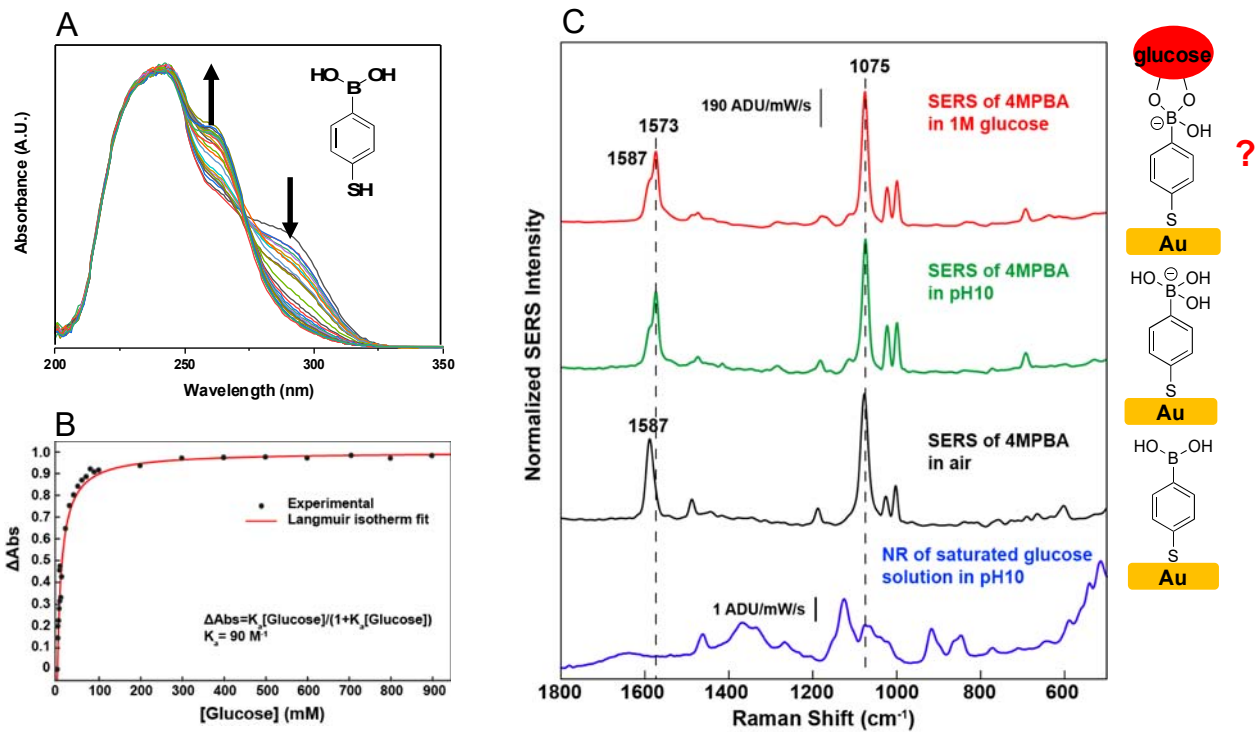


**Figure 5. 4-MPBA binding interaction with glucose (A-B) in solution using UV-visible spectroscopy and (C) on a plasmonic substrate surface using SERS.** (**A**) UV-vis spectra of 4-MPBA as change in glucose concentration 10% EtOH/pH 10 buffer, (**B**) Langmuir isotherm of 4-MPBA binding interaction with glucose, (**C**) SERS spectrum of 4-MPBA on a AuNR substrate before and after adding saturated glucose solution in pH 10 buffer. SERS spectra were normalized to the peak at 1075 $cm^{-1}$ and are an average of seven spectra collected using a 20x ELWD objective, $P_{ex}$ = 400 μW, $\lambda_{ex}$ = 785 nm, Savitsky-Golay filtering and baseline correction).

Previous work has observed boronic acids cross-linking with other boronic acids thus preventing from glucose binding.[10,11] To address this possibility, protecting 4-MPBA with pinacol ester or adding spacer molecules was an alternative method for glucose detection.

### b. pinacol ester protected 4-MPBA

Pinacol ester protected 4-MPBA was synthesized in the Mrksich lab (**Figure 6A**). The normal Raman spectra of 4-MPBA with and without pinacol ester were taken for comparison and there were spectral differences in the lower and higher wavenumber ranges (**Figure 6A-B**). Most importantly, the normal Raman of pinacol ester protected 4-MPBA showed an aliphatic C-H stretch at 2979 $cm^{-1}$, which was evidence for pinacol ester. We then immobilized pinacol ester protected 4-MPBA on a SERS substrate, removed pinacol ester by hydrolysis, and introduced concentrated glucose solution. Similar to 4-MPBA, a shoulder peak near 1576 $cm^{-1}$ appeared after incubating the substrate in pH 10 buffer (**Figure 7**). However, there was no direct or indirect evidence of glucose binding when the saturated glucose solution was introduced.

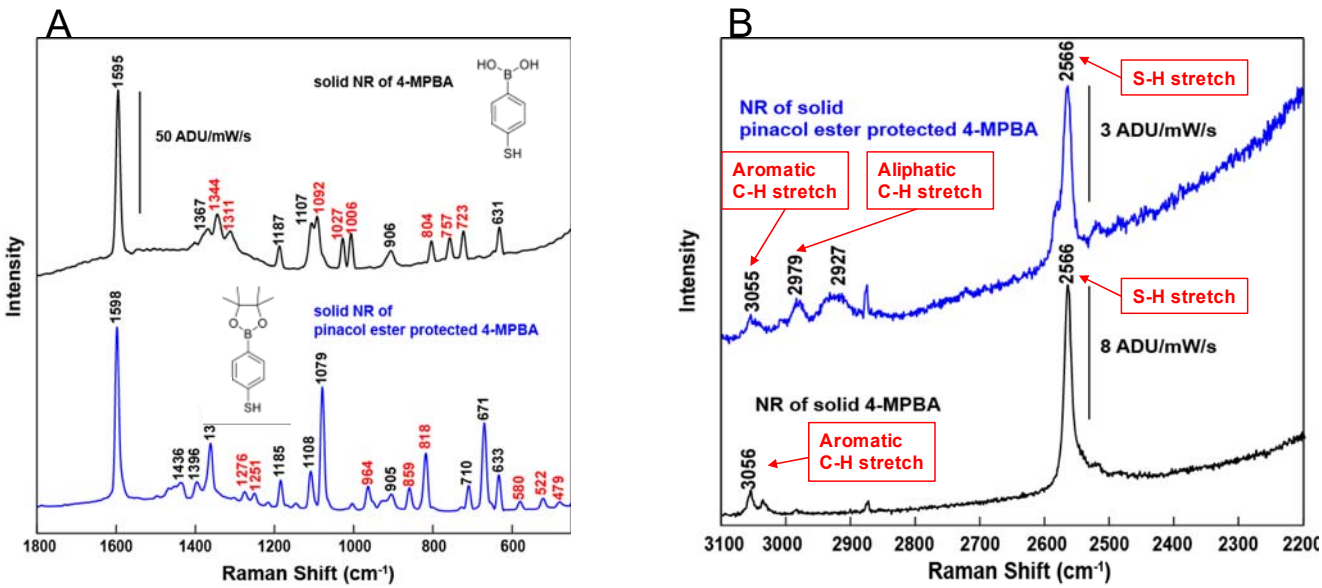


**Figure 6. Normal Raman of solid 4-MPBA and pinacol ester protected 4-MPBA in the (A) lower and (B) high wavenumber range** ($\lambda_{ex}$ = 785 nm, 20x ELWD objective, $P_{ex}$ = 3 mW, $t_{aq}$ = 1 min).

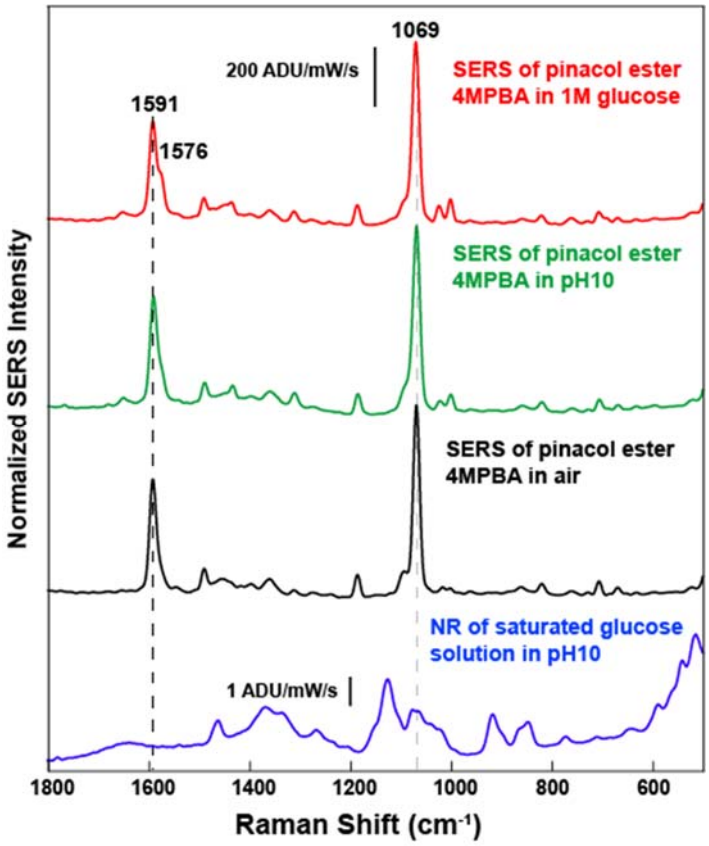


**Figure 7. SERS spectra of pinacol ester protected 4-MPBA functionalized on SERS substrate for glucose sensing after removing piancol ester** (from bottom to top: normal Raman of saturated glucose solution in pH 10, SERS of pinacol ester protected 4-MPBA in air, in pH 10, and in 1M glucose solution in pH 10, average of seven spectra collected using 20x ELWD objective, $P_{ex}$ = 400 μW, $t_{aq}$ = 1 min, $\lambda_{ex}$ = 785 nm, Savitsky-Golay filtering and baseline correction).

### c. Spacer molecules for preventing cross-linking between boronic acids

As an alternative method to solve the challenge of cross-linking between PBAs on the plasmonic nanomaterial surface, we tried a mixed self-assembled monolayer (SAM) consisting of various thiol molecules acting as a spacer molecule and 4-MPBA as the glucose capture ligand. We chose alkanethiols (octanethiol and decanethiol), adamantanethiol, benzenethiol (BZT), and mercaptobenzoic acid (4-MBA) as spacer molecules and varied the ratio between the spacer molecule and 4-MPBA on a SERS substrate. After functionalizing a mixed SAM (a spacer molecule and 4-MPBA) on a SERS substrate, Au film-over-nanospheres (AuFON), at various ratios, we incubated them in pH 10 buffer and then in a saturated glucose solution in a flow cell. The resulting SERS spectra showed no change in peak position or new peaks. Although we observed both the spacer molecule and 4-MPBA functionalized on AuFON with SERS, the spacer molecules were not optimal for promoting glucose binding. To eliminate the possibility of PBAs cross-linking and observe glucose fingerprint when bound to 4-MPBA as a reference, the Mrksich lab synthesized a complex where two 4-MPBA molecules bonded to one glucose molecule.

### d. 4-MPBA glucose complex

To fundamentally understand the binding interaction of 4-MPBA with glucose to try to answer the question of why we observe evidence that 4-MPBA binds glucose in solution via UV-vis spectrophotometry, but we cannot detect that binding via SERS, we investigated a complex where 4-MPBA was pre-bound to glucose (**Figure 8A**). The NMR of the complex showed the evidence of glucose directly bound to two 4-MPBA molecules. Additionally, there was a broad peak at 2926 $cm^{-1}$ in the normal Raman spectrum of the solid, possibly representing glucose (**Figure 8B**).

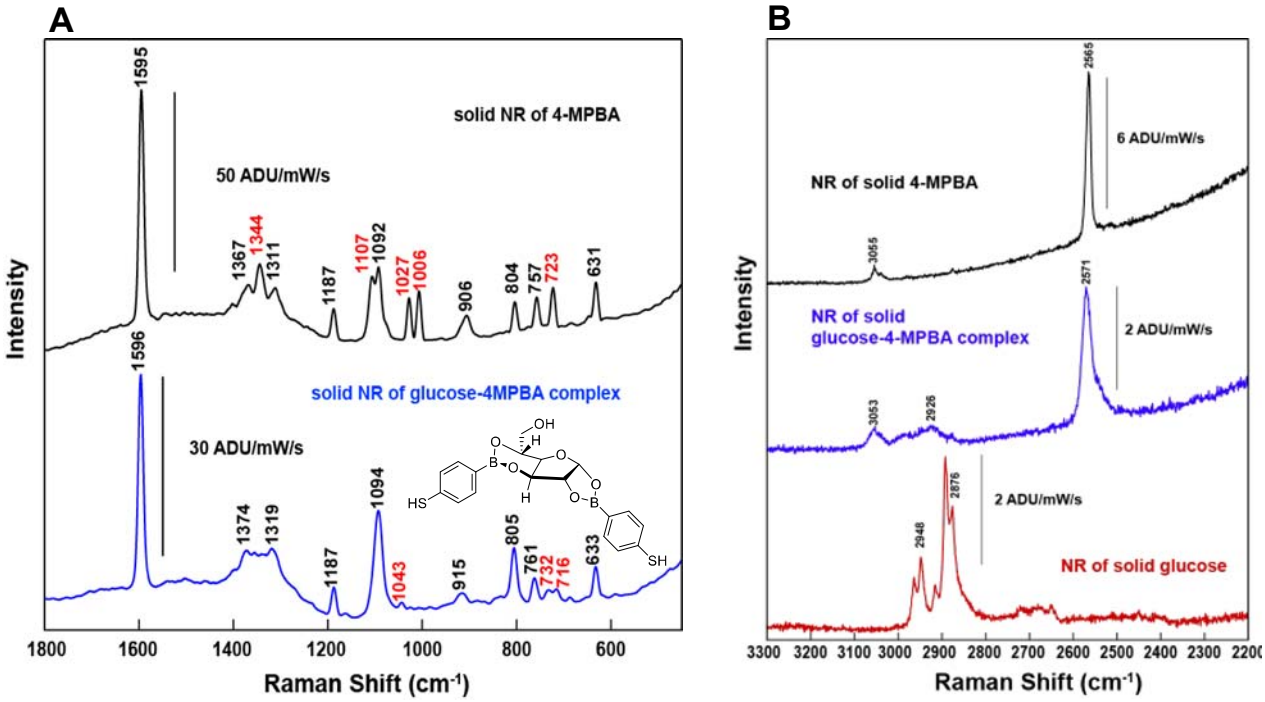


**Figure 8. Normal Raman of solid 4-MPBA and glucose-4-MPBA complex in the (A) lower and (B) higher wavenumber range with solid glucose normal Raman** ($\lambda_{ex}$ = 785 nm, 20x ELWD objective, $P_{ex}$ = 8 mW, t = 1 min).

Then we functionalized a SERS substrate with the complex and SERS spectra were collected in air (**Figure 9**). We used anhydrous ethanol to dissolve the complex and incubate our SERS substrate to prevent glucose possibly detaching from 4-MPBA by hydrolysis of the boronate groups. The resulting SERS data did not show the dominant glucose peak expected around ~1126

$cm^{-1}$ based on the normal Raman of glucose or any other direct evidence. The substrate was then rinsed with water to remove glucose in the complex by hydrolysis. Similar to 4-MPBA SERS data, a new peak at 1572 $cm^{-1}$ appeared. This result only showed the evidence of the tetrahedral form of 4-MPBA, but not a direct or indirect evidence of glucose. We hypothesize that either glucose bound on the complex dissociated when the complex was functionalized on the surface or glucose molecule is a weak Raman scatterer that we cannot not observe with SERS.

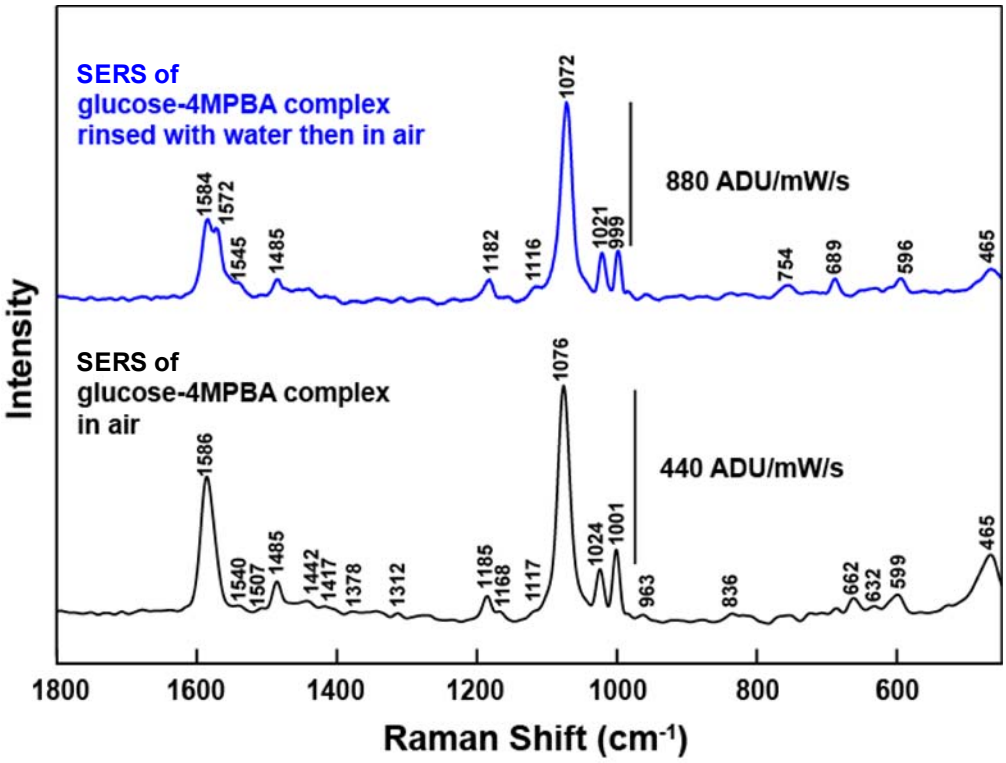


**Figure 9. SERS glucose-4-MPBA complex functionalized on a SERS substrate measured in air (black) and after rinsing with water (blue)** (Average of seven spectra using 20x ELWD objective, $P_{ex}$ = 400 μW, t = 1 min, $\lambda_{ex}$ = 785 nm, with Savitsky-Golay filtering and baseline correction).

### e. Direct glucose sensing with SERS using thiolated glucose (1-Thio-β-D-glucose sodium salt)

Because we did not observe any direct evidence of glucose, we postulated that it could be due to the relatively low Raman cross section of glucose, rather than a problem of the capture ligands not binding glucose. To investigate this possibility, we tried detecting 1-thio-β-D-glucose sodium salt (thiolated glucose) with SERS. Thiolated glucose will form a gold-thiolate bond, eliminating the distance dependence issue and the requirement for a capture ligand (as glucose itself does not adsorb to metal surfaces) Our hypothesis is that if we could directly detect glucose using SERS, the difficulty in glucose detection can be narrowed down to the glucose capture ligands. Thus, SERS spectrum was taken after functionalizing thiolated glucose onto a SERS substrate. We observed the SERS of thiolated glucose as shown in **Figure 10**. The SERS spectrum matched the normal Raman, the SERS data in the literature[12], and the DFT calculation of thiolated glucose. Therefore, it appears that the barrier to detecting glucose by SERS is most likely the efficacy of the capture agents to bind glucose when the capture agents are immobilized on a surface. To investigate the capture ligand for glucose binding on surface, we then tried a sandwich assay where we added another PBA that could bind to the other side of glucose with a distinct Raman fingerprint.

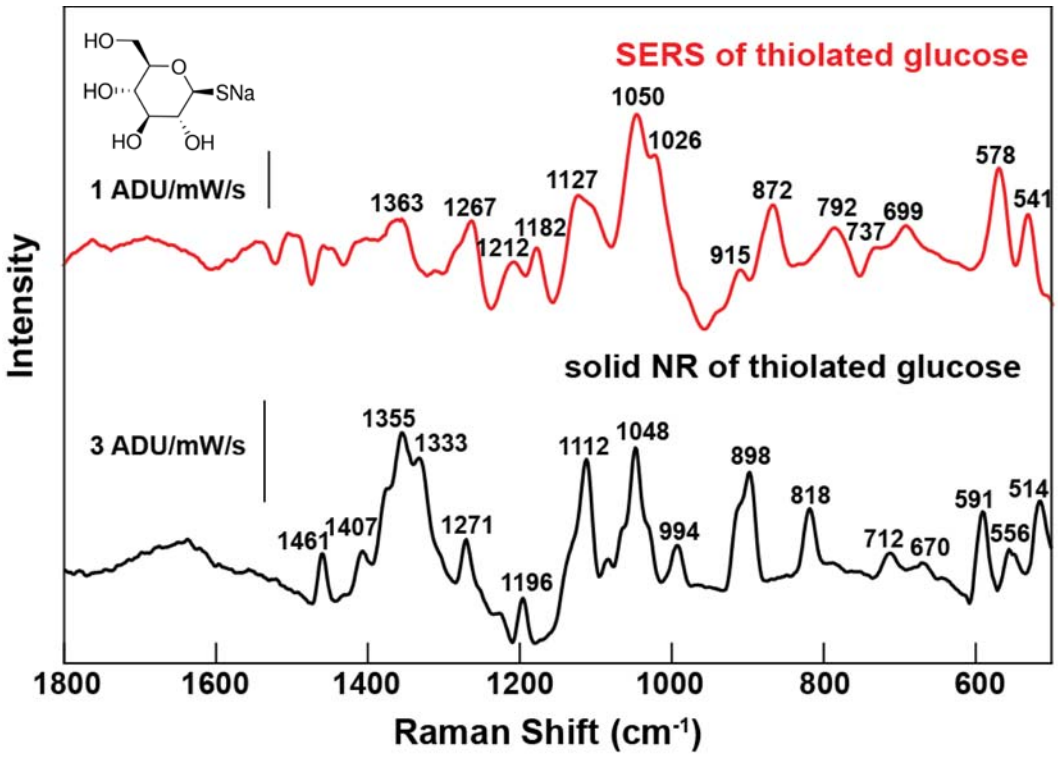


**Figure 10**. **SERS of thiolated glucose functionalized on a SERS substrate and the normal Raman of thiolated glucose measured with a macro Raman set-up** ($\lambda_{ex}$ = 785 nm, $P_{ex}$ = 3 mW for normal Raman and 30 mW for SERS, $t_{aq}$ = 3 min, with Savitsky-Golay filtering and baseline correction).

### f. Sandwiching glucose between two boronic acids

It is reported that PBAs reversibly bind with cis-1,2- or 1,3-diols.[9] Among various configurations of glucose at equilibrium, one glucose configuration has two syn-periplanar diols that could potentially bind with two PBAs (**Figure 11**).[9] With two pairs of syn-periplanar diols for glucose, Chen et al. detected glucose using a sandwich assay where 4-MPBA on the surface bond with one of glucose diols and 4-cyanophenylboronic acid (4-CPBA) bond with the diols on the other side.[13] Since the cyano group has a Raman peak at around 2200 $cm^{-1}$, they were able to observe the CN mode in the resulting SERS spectrum. Thus, we tried capturing glucose by sandwiching the molecule in between 4-MPBA functionalized on SERS substrate and 4-CPBA. However, there was no direct or indirect evidence of glucose or indication of CN mode in the resulting SERS spectrum. A possible reasoning for not observing the CN mode is that the glucose configuration consists of two syn-periplanar form is present at a small percentage (~0.14%) of the total configurations.


**Figure 11**. **Glucose configurations in the dominant form (left) and the form with two syn-periplanar diols (right)**.[9]

We tested 4-MPBA binding interaction with molecules with diols, such as fructose. Surprisingly, the binding constant of 4-MPBA with glucose in solution was similar to that of fructose obtained by UV-visible titration study. According to the literature, the binding constant should be about 40 times higher for fructose than that of glucose.[9] Although we observed a binding trend of 4-MPBA for glucose, we could not observe a direct or indirect evidence of glucose detection. Recently, there was a report where UV-vis titration study of porphyrin with glucose showed a binding trend similar to that of 4-MPBA with glucose, but they did not observe a direct evidence of glucose binding to the porphyrin.[14] They mentioned that the binding trend from the UV-vis titration study could be due to aggregation of the capture ligand, not from the binding.

### 3.2. Optimization of NOA microneedles for SERS biosensing and developing a method to localize AuNRs at microneedles tips

AuFONs prepared by the **Van Duyne** group are very important initial standards for plasmonic (hydrogel or NOA) microneedles to identify the maximum Raman signal intensity of the reporter molecules. Thus, we can adjust the plasmonic microneedles patch formulation in a way that the SERS signal can be maximized for biosensing applications. Previously shown SERS spectra of the reporter molecule demonstrated the dominant Raman fingerprints. However, the Raman signal intensities were not as high as the AuFONs samples. In order to improve the SERS activity of plasmonic NOA microneedles, we prepared the plasmonic patches with different capture ligand density on the particles surface. This could be done by simply working with varied capture ligand concentration ranging from 10 to 100 mM and their extended incubation time (24 h) compared to earlier samples (45 min). We observed enhanced SERS signals for the samples that hold higher ligand density (**Figure 12**).

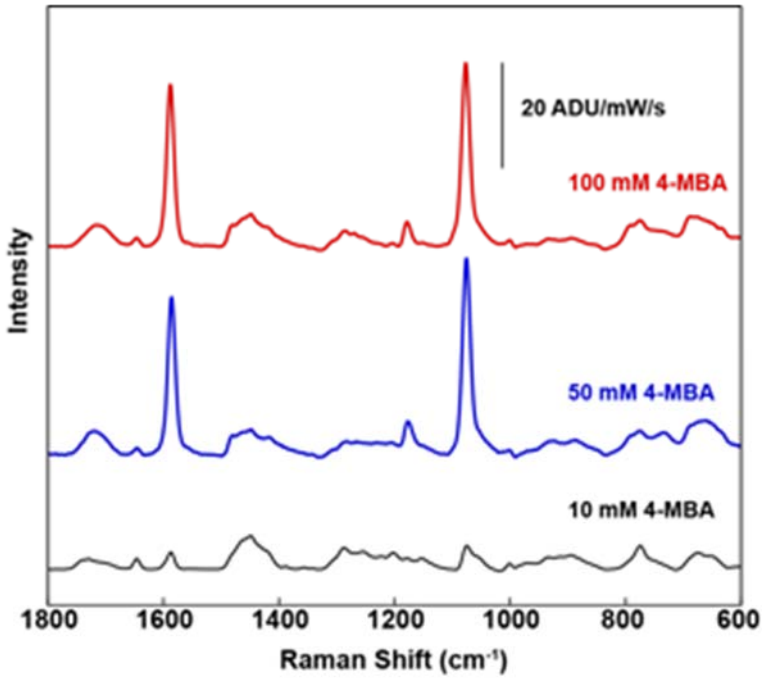


**Figure 12. Enhanced SERS activity of plasmonic NOA microneedles by tuning Raman reporter molecule (4-mercaptobenzoic acid) density on AuNRs surface.** (20x ELWD objective, $\lambda_{ex}$ = 785 nm, $P_{ex}$ =1 mW, Savitsky-Golay filtering and baseline correction).

Tip sections of the transdermal plasmonic patches will be interacting with interstitial fluid upon piercing into skin. Once the light source is focused on the plasmonic device, Raman fingerprints of glucose-captured ligands will be collected from a large area across the surface that is limited by the laser spot size. Alternatively, the laser can be scanned across the device surface and the Raman signals

of the reporter molecule can be averaged for a given area. In this scenario, capture ligand Raman signals originated from the flat regions between microneedles tips would give background signals of un-bound ligands given the fact that flat regions are not in direct contact with epidermis and interstitial fluid. The best way to differentiate bound *vs* unbound capture ligand signals is to localize plasmonic component selectively at the tips surface and to minimize the particles density on the flat regions. This will allow us to maximize the sensing performance of the plasmonic microneedles. In order to prepare selective particle entrapment only within the hydrogel tip or deposition on the NOA tip surface, we have tried a few different approaches:

**(i) Au NRs localization at the Gantrez-PEG microneedles tips:** Pre-polymer solution of Gantrez and PEG was mixed with AuNRs following its deposition on the PDMS mold. The excess solution was carefully removed from the mold surface by wiping with a glass slide. The mixture was allowed to dry for a few hours at ambient conditions. Then, the mold was filled with the same hydrogel mixture composition but without AuNRs and polymerized at high temperature. In **Figure 13**, optical images of the resulting sample demonstrate AuNRs that are localized at the microneedles tips. Following the capture ligand immobilization on particles surface, SERS activity was measured as maximized at the hydrogel microneedles tip only (**Figure 13D**).

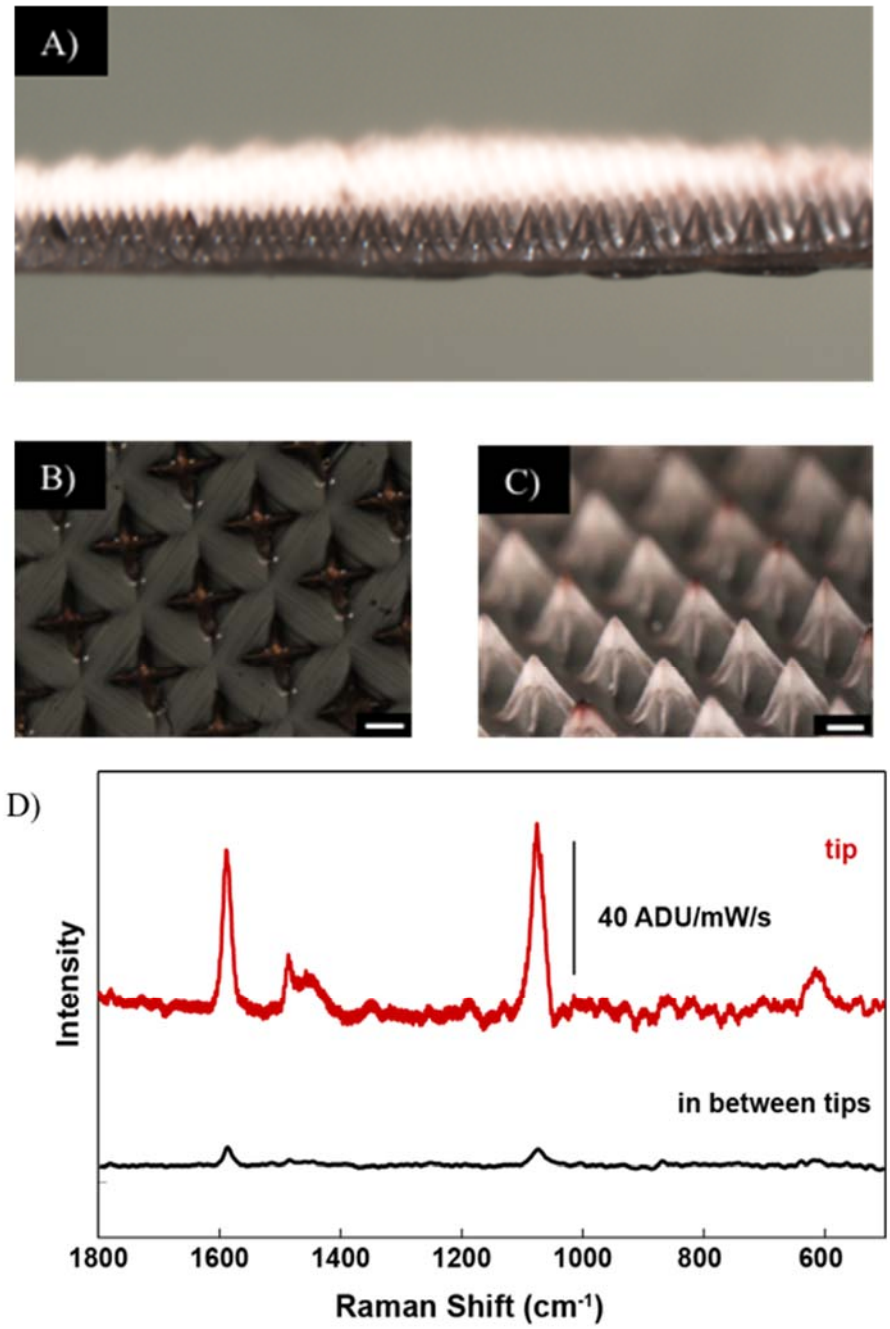


**Figure 13. Localized AuNRs at plasmonic-PEG microneedles tips and corresponding SERS activity.** Optical images of an array of plasmonic Gantrez-PEG hydrogel microneedles with AuNRs selectively localized at the tips: (A) in large field of view, (B) from top view, and (C) from tilted sample. Scale bars are 200 mm. (D) SERS spectra of 4-MPBA at the plasmonic Gantrez-PEG hydrogel tip (red) and flat regions in between the microneedles (black) (20x ELWD objective, $\lambda_{ex}$ = 785 nm, $P_{ex}$ = 0.55 μW, Savitsky-Golay filtering and baseline correction).

**(ii) Au NRs localization at the NOA microneedles tips:** A drop of AuNRs solution was deposited on a flat PDMS surface and let dry. Then, particles were transfer printed on the NOA microneedles tip by bringing the PDMS in contact with the microneedles. AuNRs were transferred from the PDMS surface onto the tips (**Figure 14A-B**). Once the patch was incubated in the reporter molecule solution, particles remained intact giving strong SERS signals (**Figure 14C**).

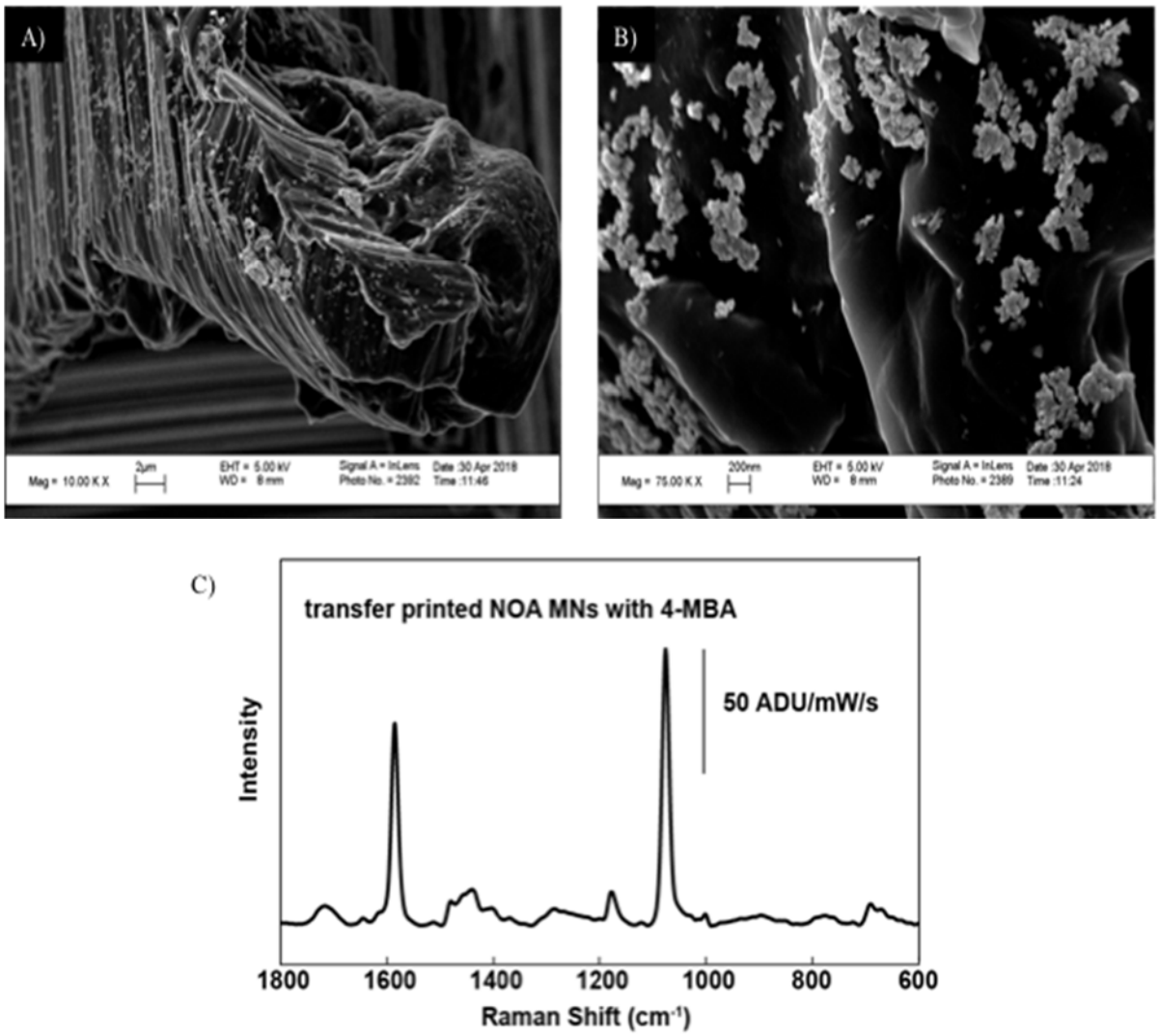


**Figure 14. Localized SERS activity on plasmonic NOA microneedles tips.** (A, B) SEM micrograph of transfer printed Au NRs assembly localized at NOA microneedles tip. (C) SERS activity of transfer printed samples demonstrating localized SERS signals at the microneedles tips (20x ELWD objective, $\lambda_{ex}$ = 785 nm, $P_{ex}$ =1 mW, Savitsky-Golay filtering and baseline correction).

We were concerned with the possibility of partial ligand exchange during the ligand immobilization step where AuNRs were already aggregated on the NOA surface and capture ligand molecules may not diffuse in depth of the randomly arranged particles aggregates due to tight particle-particle contacts. This will strongly reduce the number of SERS active hot spots for the signal enhancement and will lead to reduced signal-to-noise ratio. We came up with an alternative approach to maximize SERS signals. In this approach, AuNRs assembly on the NOA microneedles as well as their functionalization with capture ligand were performed in situ while NOA patch was incubated in the mixture of particles and capture ligand solution (**Figure 15**). Since this is another solution based particle immobilization method, it does not provide selective particle deposition at the microneedles tip.

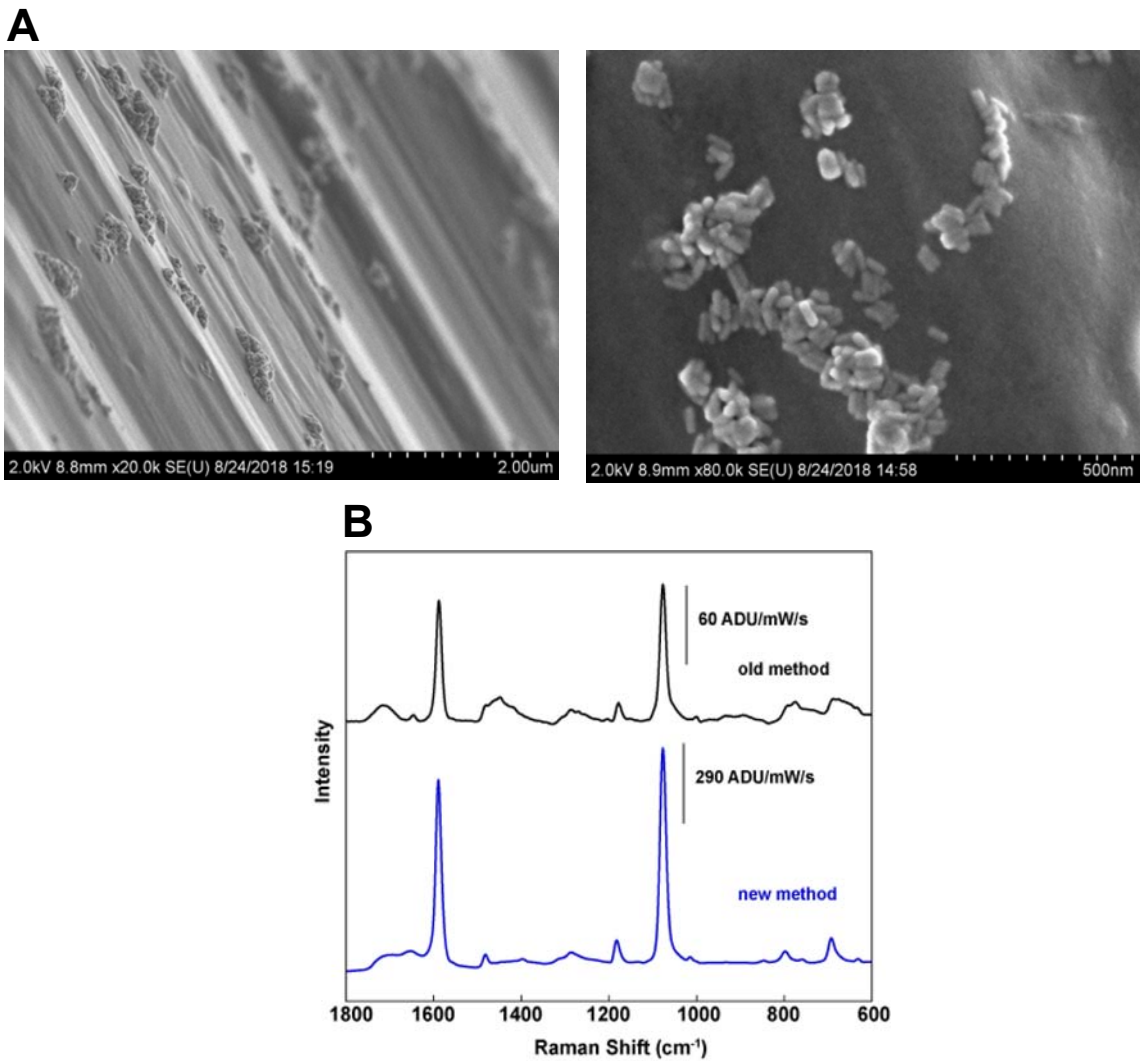


**Figure 15. In Situ AuNRs assembly and their functionalization as localized on the NOA microneedles.** (A) SEM micrographs of Au NRs that are functionalized with capture ligand as localized on NOA microneedles surface. (B) SERS spectrum of NOA MN functionalized with 4-MBA using two different methods (old vs. new).

### 4- *Ex vivo* glucose sensing by SERS; demonstrate 3 months stability and functionality of the sensor

We started with validating the plasmonic NOA microneedles for SERS biosensing. Then, we tested the mechanical and chemical stability by puncturing the microneedles in a skin phantom.

**Validating the plasmonic NOA microneedle platform for SERS biosensing**

After successfully fabricating NOA microneedles with AuNRs, we functionalized the surface with a pH sensitive molecule, 4-MBA, to validate the NOA microneedle platform for SERS biosensing. After confirming the SERS activity of the platform, we measured SERS of NOA microneedle tips by focusing a laser directly onto the tip (not through the polymer) and then focusing through the polymer in order to check whether the laser interferes with NOA polymer. The resulting SERS spectra in **Figure 16** showed the signal-to-noise ratio of the SERS signals before and after focusing through the polymer were the same, confirming the optical transparency of the polymer and appropriateness of the material for SERS sensing.

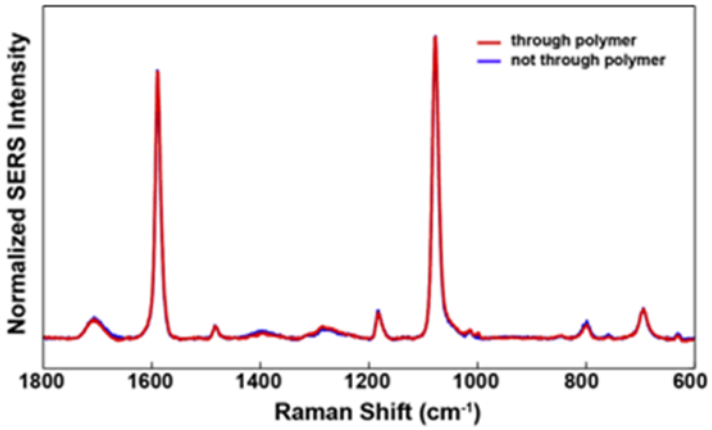


**Figure 16**. **SERS spectra of 4-MBA functionalized on AuNRs of NOA microneedles focused on the tip directly (blue) and through the NOA polymer (red)** (Average of seven spectra using 20x ELWD objective, $P_{ex}$ = 1 mW, $\lambda_{ex}$ = 785 nm, with baseline correction, and normalized to the SERS peak intensity at 1076cm$^{-1}$).

As a pH sensor, we obtained a calibration curve of the NOA microneedles by measuring SERS in Britton-Robinson buffer solutions with various pH values (pH 2-12). As the pH of the buffer solution increased, the carbonate stretching mode peak around 1400 cm$^{-1}$ increased and blue-shifted (**Figure 17**). For quantitative pH sensing, we normalized the SERS spectra to the peak intensity at 1076 cm$^{-1}$. The ratio between the integrated peak intensity at 1400 cm$^{-1}$ to 1076 cm$^{-1}$ was plotted against the pH for the calibration curve. The sensor demonstrated the pH sensitivity over the range of pH 6-9 with a $pK_a$ value of 7.26. As a comparison, 4-MBA was functionalized on AuFON, a standard SERS substrate in the **Van Duyne** lab, and a calibration curve was obtained. The $pK_a$ of 4-MBA on AuFON, determined as 7.38, was similar to that of the NOA microneedle sensor (**Figure 18A-B**). The reversibility of the pH sensing was then confirmed by measuring SERS of the microneedle sensor after randomly changing the pH of the buffer solution (Figure 11C).

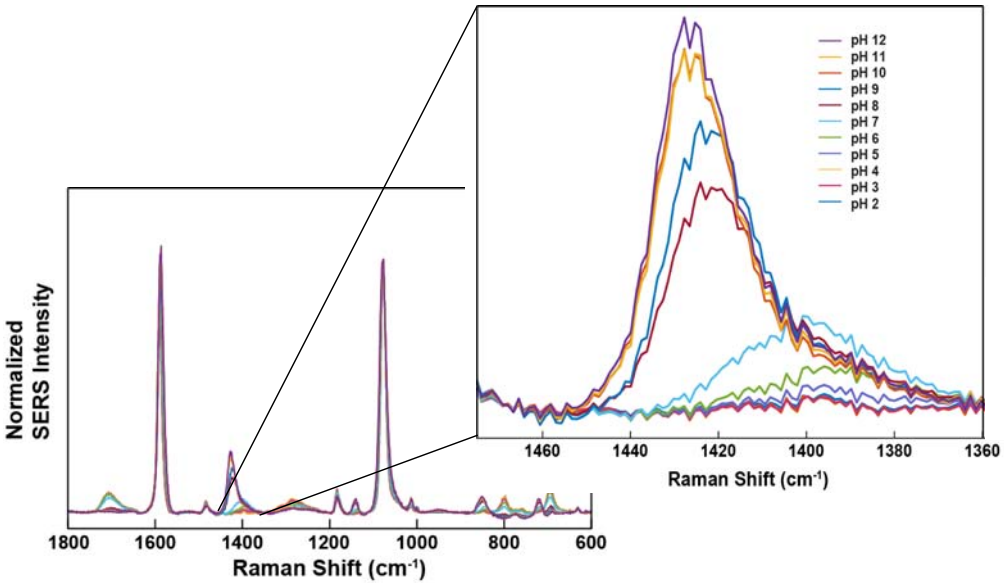


**Figure 17. Normalized SERS spectra of 4-MBA functionalized on NOA microneedles in Britton-Robinson buffer with pH range of 2-12 where laser was focused through the NOA polymer and focused on the tips** (Average of seven spectra using 20x ELWD objective, $P_{ex}$ = 1 mW, $\lambda_{ex}$ = 785 nm, with baseline correction, and normalized to the SERS peak intensity at 1076cm$^{-1}$)

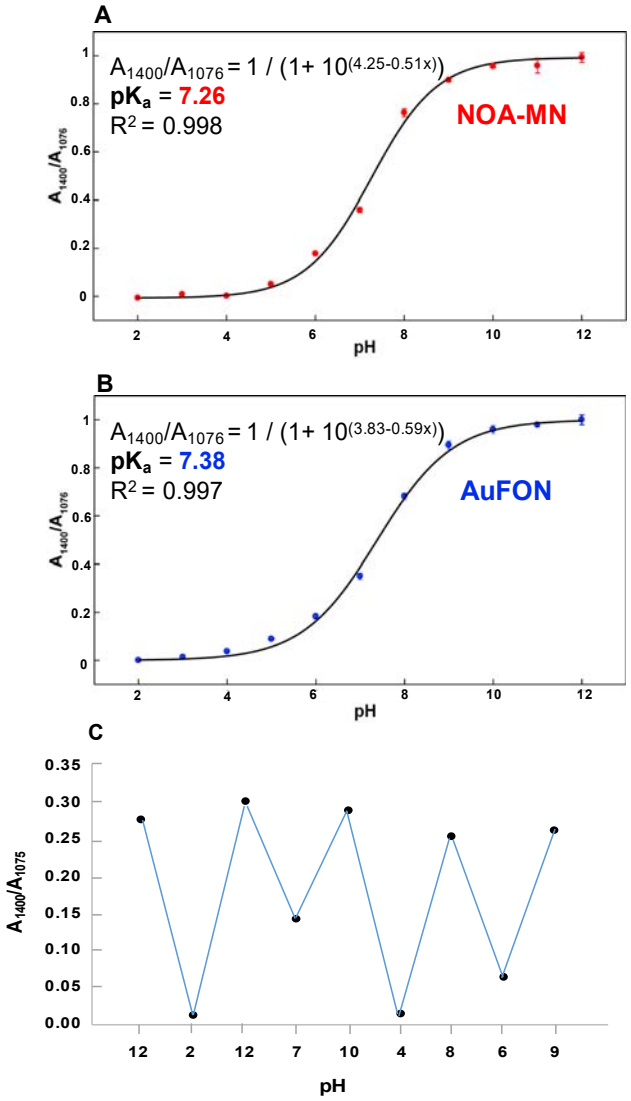


**Figure 18. pH calibration curve for (A) NOA microneedles and (B) AuFON obtained in Britton-Robinson buffer in the pH range of 2-12, and (C) reversible binding study for NOA microneedles** (Average of seven spectra using 20x ELWD objective, $P_{ex}$ = 1 mW, $\lambda_{ex}$ = 785 nm, with baseline correction, and normalized to the SERS peak intensity at 1076cm$^{-1}$).

Mechanical robustness of the sensor was demonstrated by penetrating through an agarose skin phantom and detecting the pH of the gel, and puncturing through the gel multiple time (10 times). First, NOA microneedles was punctured through an agar gel and SERS was measured while the microneedles of the sensor was in the gel. As shown in **Figure 19,** a peak at around 1400 cm$^{-1}$ increased upon inserting the microneedles into the agar gel. Based on the peak intensity at 1400 cm$^{-1}$, the pH of the agar gel was around 8. Then, the sensor was taken out from the gel and SERS was measured again after rinsing with water. The resulting SERS spectrum before and after penetrating agar gel were the same, showing the reversibility of the sensor. Lastly, SERS of the microneedle sensor was measured before and after puncturing through an agar gel 10 times (**Figure 20B**). The SERS signal intensity did not change upon penetrating the agar gel, demonstrating the mechanical stability of the sensor.

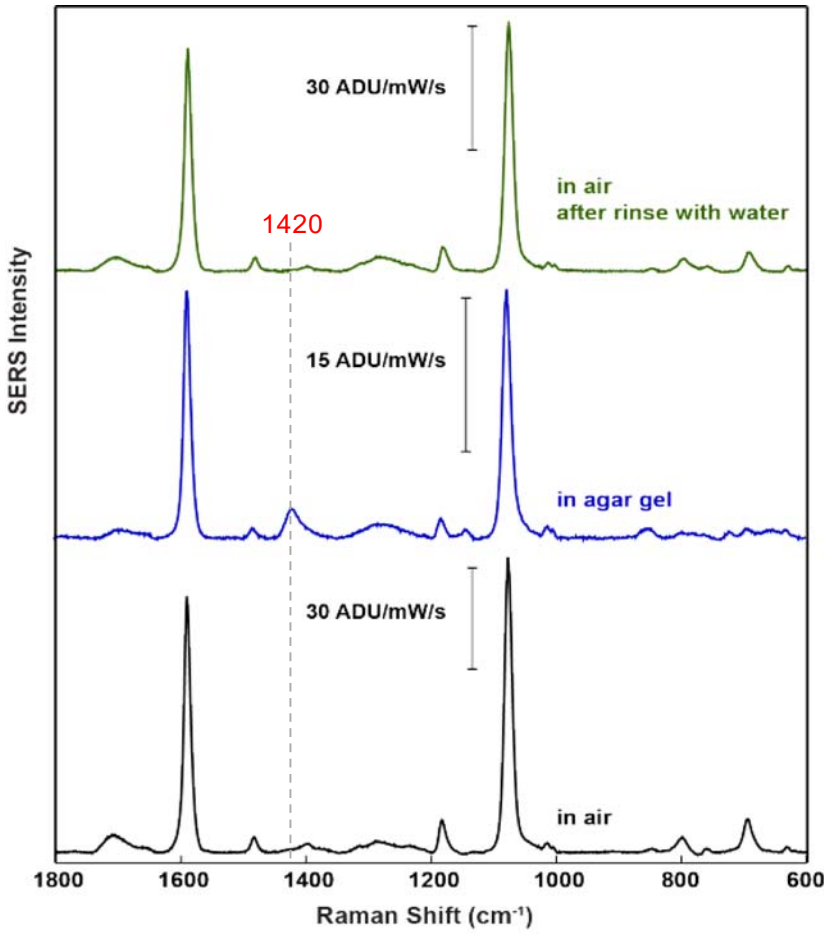


**Figure 19. SERS spectra of NOA microneedles functionalized with 4-MBA taken in air (black), agar gel (blue), air after rinsing it with water (green)** (Average of seven spectra using 20x ELWD objective, $P_{ex}$ = 1 mW, $\lambda_{ex}$ = 785 nm, with baseline correction, and normalized to the SERS peak intensity at 1076 $cm^{-1}$).

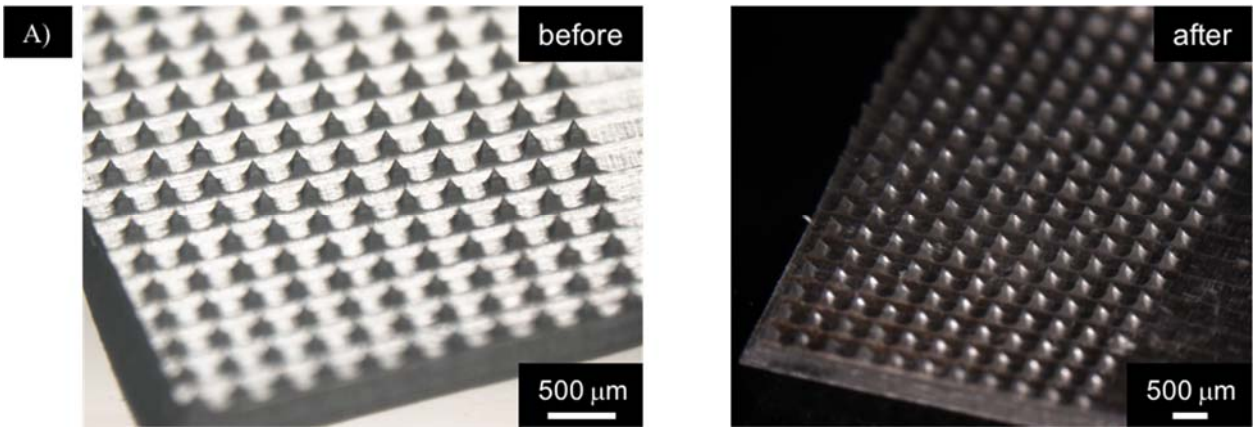

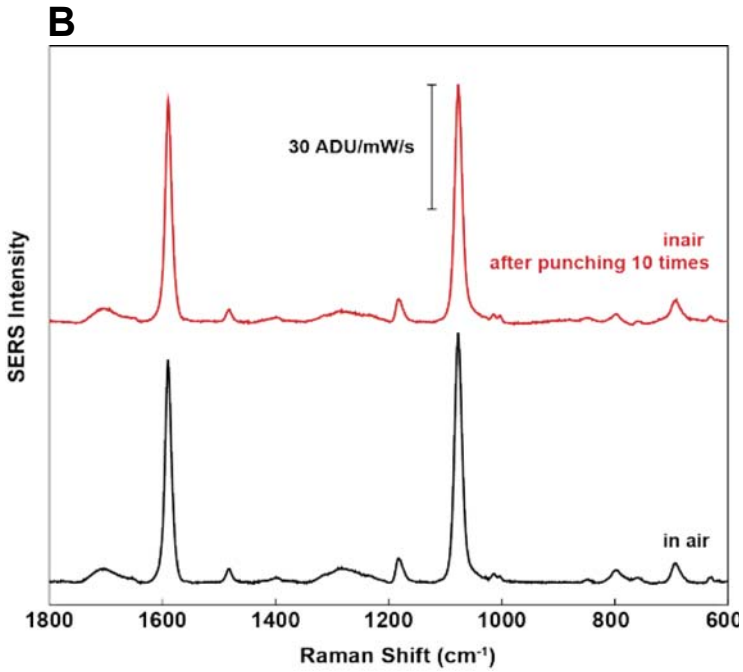


**Figure 20. Mechanical stability of plasmonic NOA microneedles upon skin insertion mimicking punching test.** (A) Optical images before and after puncture and (B) SERS activity spectra of plasmonic NOA microneedles before and after punching test (Average of seven spectra using 20x ELWD objective, $P_{ex}$ = 1 mW, $\lambda_{ex}$ = 785 nm, with baseline correction, and normalized to the SERS peak intensity at 1076cm$^{-1}$).

In conclusion, the plasmonic NOA microneedle platform has shown promising results as a transdermal pH biosensor. Ultimately, by decorating the surface with different biomolecule capture ligands, this microneedle sensor has the potential as transdermal nanosensor to monitor various physiologically relevant bioanalytes.

**References:**

(1) Donnelly, R. F.; Raghu, T.; Singh, R.; Zaid, A.; Mccrudden, M. T. C.; Neill, S. O.; Mahony, C. O.; Armstrong, K.; Mcloone, N.; Kole, P.; et al. Hydrogel-Forming Microneedle Arrays Exhibit Antimicrobial Properties : Potential for Enhanced Patient Safety. *Int. J. Pharm.,* **2013**, *451* (1–2), 76–91.

(2) Donnelly, R. F.; McCrudden, M. T. C.; Alkilani, A. Z.; Larrañeta, E.; McAlister, E.; Courtenay, A. J.; Kearney, M. C.; Raj Singh, T. R.; McCarthy, H. O.; Kett, V. L.; et al. Hydrogel-Forming Microneedles Prepared from "Super Swelling" Polymers Combined with Lyophilised Wafers for Transdermal Drug Delivery. *PLoS One.,* **2014**, *9* (10).

(3) Wirth, M.; Arangoa, M. A.; Gabor, F.; Irache, J. M. Gantrez AN as a New Polymer for the Preparation of Ligand – Nanoparticle Conjugates. *J. Control Release*., **2002**, *83*, 321–330.

(4) Ojer, P.; Cerain, A. L. De; Areses, P.; Peñuelas, I.; Irache, J. M. Toxicity Studies of Poly ( Anhydride ) Nanoparticles as Carriers for Oral Drug Delivery. *Pharmaceutical Research*. **2012**, *29*, 2615–2627.

(5) Biedma, B. M.; Martín, B. Amoxicillin-Loaded Sponges Made of Collagen and Poly [( Methyl Vinyl Ether ) -Co- ( Maleic Anhydride )] for Root Canal Treatment : Preparation , Characterization and In Vitro Cell Compatibility. *J. Biomater. Sci. Polym. Ed.,* **2012**, *5063*.

(6) Moreno, E.; Schwartz, J.; Larra, E.; Nguewa, P. A.; Sanmartín, C.; Agüeros, M.; Irache, J.

M.; Espuelas, S. Thermosensitive Hydrogels of Poly ( Methyl Vinyl Ether-Co-Maleic Anhydride ) – Pluronic ® F127 Copolymers for Controlled Protein Release. *Int. J. Pharm*. **2014**, *459*, 1–9.
(7) Masango, S. S.; Hackler, R. A.; Large, N.; Henry, A.; Mcanally, M. O.; Schatz, G. C.; Stair, P. C.; Duyne, R. P. Van. High-Resolution Distance Dependence Study of Surface-Enhanced Raman Scattering Enabled by Atomic Layer Deposition. *Nano Lett.*, **2016**, *16(7)*, 4251-4259.
(8) Wiig, H.; Swartz, M. A. Interstitial fluid and lymph formation and transport : physiological regulation and roles in inflammation and cancer. *Physiol. Rev*., **2012**, *92(3)*, 1005–1060.
(9) Wu, X.; Li, Z.; Chen, X. X.; Fossey, J. S.; James, T. D.; Jiang, Y. B. Selective Sensing of Saccharides Using Simple Boronic Acids and Their Aggregates. *Chem. Soc. Rev.,* **2013**, *42* (20), 8032–8048.
(10) Li, S.; Zhou, Q.; Chu, W.; Zhao, W.; Zheng, J. Surface-Enhanced Raman Scattering Behaviour of 4-Mercaptophenyl Boronic Acid on Assembled Silver Nanoparticles. *Phys. Chem. Chem. Phys.* **2015**, *17,* 17638-17645.
(11) Torul, H.; Çiftçi, H.; Dudak, F. C.; Adıgüzel, Y.; Kulah, H.; Boyacı, İ. H.; Tamer, U. Glucose Determination Based on a Two Component Self-Assembled Monolayer Functionalized Surface-Enhanced Raman Spectroscopy (SERS) Probe. *Anal. Methods* **2014**, *6* (14), 5097–5104.
(12) Vezvaie, M.; Brosseau, C. L.; Goddard, J. D.; Lipkowski, J. SERS of Beta-Thioglucose Adsorbed on Nanostructured Silver Electrodes. *Chemphyschem : a European journal of chemical physics and physical chemistry*., **2010**, *11*, 1460-1467.
(13) Chen, Q.; Fu, Y.; Zhang, W.; Ye, S.; Zhang, H.; Xie, F.; Gong, L.; Wei, Z.; Jin, H.; Chen, J. Highly Sensitive Detection of Glucose: A Quantitative Approach Employing Nanorods Assembled Plasmonic Substrate. *Talanta.,* **2017**, *165*, 516-521.
(14) Renney, C. M.; Fukuhara, G.; Inoue, Y.; Davis, A. P. Binding or Aggregation? Hazards of Interpretation in Studies of Molecular Recognition by Porphyrins in Water. *Chem. Commun.,* **2015**, *51*, 9551-9554.

**Opportunities for training and professional development provided by the project**

Ji Eun Park joined the Van Duyne group in September 2016 as a second-year graduate student. She was trained in AuFONs fabrication, LSPR and SERS characterization, including EF measurement. She is now fully trained and operational for working independently in the lab on the experiments relevant to this program.

Other team members were already trained in their field of expertise.

**Dissemination of results to communities of interest**

Ji Eun Park took part in the 'All Scout Nanoday' outreach event organized by the International Institute for Nanotechnology and hosted in part by the Van Duyne lab. They engaged with a young audience (~10-14 year-old girl and boy scouts from the Chicago area) to communicate about nanotechnology research and careers in science.

**Plan for the next reporting period towards accomplishing outlined goals**

The Van Duyne group and the Mrksich group are currently working on a manuscript for publishing the results of the NOA microneedle sensor for pH sensing.

The Van Duyne group will continue working on optimizing both the Gantrez-PEG- and NOA-based microneedles for SERS biosensing and localizing AuNRs on the microneedle tips. The Mrksich group will continue synthesizing and evaluating various glucose capture ligands with highest binding and selectivity.

Both groups will keep working on evaluating various glucose-capture layer binding in solution but most importantly on metal surfaces, as well as measuring SERS spectra and quantifying glucose concentration. Finally, since we successfully fabricated plasmonic NOA microneedles for SERS biosensing application, we will integrate the glucose capture ligand to the microneedle sensor. We will then test through skin and evaluate the stability in a complex biofluid. Using our animal studies protocol, which has been approved by our IACUC and submitted to ACURO for approval, we can test the efficiency of the sensor *in vivo* in the near future.

4. IMPACT

**Impact on the development of the principal discipline(s) of the project**

The development of plasmonically active polymer platforms is new when applied to combining microneedles and SERS. As such, this project presents an exciting new area of research to pursue, at the nexus of organic and analytical chemistries, materials science, and biomedical engineering. Both research groups are closely and actively pursuing the development of these new functional platforms. We anticipate publishing our findings in a scientific publication this year and another over the next reporting period.

**Impact on other disciplines**

Nothing to report.

**Impact on technology transfer**

Nothing to report yet. An invention disclosure will be submitted to Northwestern's Innovation and New Ventures Office for review on patentability and marketability of the plasmonic microneedle patches once the manuscript is submitted to a peer-reviewed journal.

**Impact on society beyond science and technology**

Nothing to report.

5. CHANGES/PROBLEMS

**Changes in approach and reasons for change**

Nothing to report.

**Actual or anticipated problems or delays and actions or plans to resolve them**

Difficulties detecting glucose using small PBAs with SERS slowed down the sensing part of the project more than anticipated. Extensive effort was dedicated to synthesize, purify, characterize, and scale up the custom-syntheses for PBA-based glucose capture ligands. We have investigated several PBA-based ligands as shown in Table 1 for glucose sensing efficiency. The results will potentially lead to finding different glucose capture ligands and possibly determining other bioanalytical targets

for the working microneedle sensor. We will continue to investigate other glucose capture ligands to detect glucose. Meanwhile, with the working microneedle SERS sensor, we will list pH as the new target. Detecting epidermal pH is important since we can potentially monitor skin disorder and wound healing process.

**Table 1**. Boronic acid-based ligands evaluated for glucose detection.

| Molecule | |
|---|---|
| **mono boronic acid** (4-MPBA with and without pinacol ester protection) | 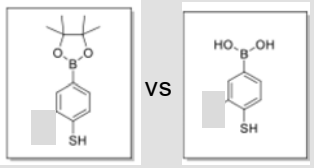 |
| **Fluorinated 4-MPBA** | 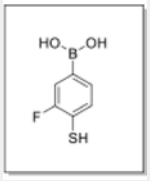 |
| **Glucose 4-MPBA complex** | 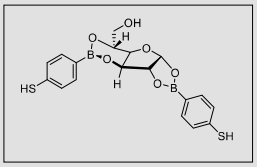 |
| **1,1-BBA and 2,2-BBA** | 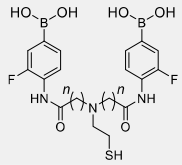 |

**Changes that had a significant impact on expenditures**

Nothing to report.

**Significant changes in use or care of human subjects, vertebrate animals, biohazards, and/or select agents**

Nothing to report.

6. PRODUCTS

**Publications, conference papers, and presentations**

- **Journal publications**
  J. Park, N. Y. Tanyeri, E. R. Vander Ende, A. Henry, E. Berns, M. Mrksich, R. P. Van Duyne, in preparation (2018)

- **Books or other non-periodical, one-time publications**

  Nothing to report.

- **Other publications, conference papers, and presentations**

- Dr. Nihan Yonet-Tanyeri presented her work with a poster presentation on the Society for Biomaterials (SFB) Biomaterials Day at the University of Michigan-Ann Arbor, MA in October 2017 entitled "SERS Based Transdermal Patches for Nanosensing."

- Dr. Nihan Yonet-Tanyeri was also invited to give an oral presentation at the Annual Meeting of American Institute of Chemical Engineers (AIChE, October 28 - November 2, 2018) that will be held in Pittsburgh, PA. Her talk is entitled "Non-invasive Plasmonic Biosensors for In Situ Glucose Monitoring."

- **Website(s) or other Internet site(s)**

  A brief description of the SERS-enabled biosensing efforts in the Van Duyne lab is provided on the group webpage:
  http://sites.northwestern.edu/vanduyne/research/sers-biosensing/

  Direct access to previously cited publications is also provided on the website:
  http://sites.northwestern.edu/vanduyne/publications/

- **Technologies or techniques**

  Plasmonic microneedles described in Accomplishments are technologies directly resulting from this program.

- **Inventions, patent applications, and/or licenses**

  Nothing to report.

- **Other Products**

  Nothing to report.

7. PARTICIPANTS AND OTHER COLLABORATING ORGANIZATIONS

- **Individuals working on the project**

| | |
|---|---|
| Name: | *Richard Van Duyne (no change)* |
| Name: | *Milan Mrksich (no change)* |
| Name: | *Ji Eun Park (no change)* |
| Name: | *Emma Vander Ende (no change)* |
| Name: | *Anne-Isabelle Henry (left in March 2018)* |
| Name: | *Pradeep Bugga (no change)* |
| Name: | *Daniel Sykora (no change)* |
| Name: | *Nihan Yonet-Tanyeri (left in August 2018)* |

| | |
|---|---|
| Name: | *Eric Berns* |
| Project Role: | *Research Assistant Professor* |
| Researcher Identifier (e.g. ORCID ID): | *0000-0002-2203-0847* |
| Nearest person month worked: | *5* |
| Contribution to Project: | *Participates in regular meetings with the team and provided guidance to facilitate successful execution of project goals. He has helped evaluate binding to immobilized capture ligands on monolayers. He has aided in the development of protocols for microneedle testing. He participated in the preparation of the animal protocols for IACUC approval and the related trainings.* |
| Funding Support: | *National Institute of Health* |

| | |
|---|---|
| Name: | *Tsatsral Iderzorig* |
| Project Role: | *Research Technologist* |
| Researcher Identifier (e.g. ORCID ID): | *N/A* |
| Nearest person month worked: | *12* |
| Contribution to Project: | *Assists with materials preparation and chemical purification, ordering and stocking of supplies and performing basic lab tasks and maintenance as support for experiments.* |
| Funding Support: | *N/A* |

- **Change in the active other support of the PD/PI(s) or senior/key personnel since the last reporting period.**

  Nothing to report.

- **Other organization involved as partners**

  Organization Name: NU*ANCE*, Northwestern University
  Location of Organization: Evanston, IL
  Partner's contribution to the project: Facilities; project staff from the Van Duyne lab and Mrksich lab used Northwestern's electron microscopy facility to characterize the morphology of the microneedles platforms by scanning electron microscopy.

8. SPECIAL REPORTING REQUIREMENTS

   Since this is a collaborative award, the PI (Richard Van Duyne) and Partnering PI (Milan Mrksich) will each submit a similar report.

9. APPENDICES

   None.